Available online at www.sciencedirect.com
SCIENCE DIRECT®
ELSEVIER
International Journal of Heat and Mass Transfer 47 (2004) 4979–4994
International Journal of HEAT and MASS TRANSFER
www.elsevier.com/locate/ijhmt

Fluid flow and transport processes in a large area atmospheric pressure stagnation flow CVD reactor for deposition of thin films

G. Luo, S.P. Vanka *, N. Glumac

Department of Mechanical and Industrial Engineering, University of Illinois at Urbana-Champaign, 1206 W. Green Street, Urbana, IL 61801, USA

Received 9 January 2004; received in revised form 25 June 2004
Available online 23 August 2004

Abstract

This paper investigates a new CVD reactor geometry to deposit uniform films on large area substrates at atmospheric pressure. Calculations have been performed for a wide range of parameters to investigate the effects of inlet flow rates, substrate rotation, and height of the reactor chamber. It is seen that for some combinations of the parameters the flow above the wafer is unsteady. Effect of rounded corners on damping instabilities of the shear layers is explored. By employing the rounded corners, we have been able to reduce the RMS non-uniformity to about 1% at atmospheric pressure on a 30 cm wafer. The impinging jet geometry can be used for the deposition of thin solid films without the penalty of a vacuum system and associated equipment costs.
© 2004 Elsevier Ltd. All rights reserved.

Keywords: Computer simulation; Fluid flows; Chemical vapor deposition processes

1. Introduction

Chemical vapor deposition is widely used by micro- and optoelectronic industries to deposit thin films on a substrate. A typical CVD reactor consists of a heated substrate onto which a mixture of precursor and carrier gases is impinged. Homogeneous reactions in the gas phase and heterogeneous chemical reactions at the substrate take place, resulting in a thin film of the desired material. There are at least three types of CVD reactors that are commonly used by industry. These include stagnation flow type reactors, horizontal reactors, low pressure multi-wafer, and barrel type of reactors. Of these, the stagnation flow reactor is widely studied because of its favorable deposition characteristics. A typical stagnation flow reactor consists of a cylindrical chamber with a uniform inflow of reactants to the heated substrate and outflow from an outer annular region of the reactor (Fig. 1). The heated substrate is placed on a pedestal which is often rotated. The substrate rotation helps in increasing the uniformity of the film while also increasing the growth rate through steeper concentration gradients at the substrate.

Most stagnation flow type CVD reactors are operated at sub-atmospheric pressures in order to mitigate the buoyancy-induced flows that result from the temperature difference between the substrate and the inlet gases. Buoyancy-induced flows can create severe

* Corresponding author.
E-mail address: spvanka@uiuc.edu (S.P. Vanka).

0017-9310/$ - see front matter © 2004 Elsevier Ltd. All rights reserved.
doi:10.1016/j.ijheatmasstransfer.2004.06.012

Nomenclature

A_w	area of the wafer surface
C_p	dimensionless specific heat of the carrier gas
D	dimensionless mass diffusivity
d	diameter
$\mathbf{e}_x$	unit vector with component in the x direction
g	gravitational acceleration
Ga	Gay-Lusac number
Gr	Grashof number
h	height of the chamber
$\mathbf{I}$	unit tensor
k	thermal conductivity of carrier gas
m_{sp}	specific mass flow rate per unit wafer area
p	pressure
Pr	Prandtl number
R	radial coordinate
Re	Reynolds number
Sc	Schmidt number
Sh	Sherwood number
T	temperature
t	non-dimensional time
$\mathbf{u}$	velocity vector
V	inlet velocity of carrier gas
x	non-dimensional vertical coordinate
Y	non-dimensional concentration of precursor gas

Greek symbols

μ	dynamic viscosity
Θ	non-dimensional temperature
ρ	density of carrier gas
Ω	rotation speed

Subscripts

in	inlet
ref	at reference temperature
w	wafer
h	height of reactor chamber

non-uniformities in the growth profile, making the films useless. However, operating a system under vacuum conditions requires expensive equipment and more rugged designs of the reactor chamber. Simultaneously, wafer sizes currently used by industry have steadily increased in diameter in order to increase the number of chips produced per wafer in the batch process of semiconductor manufacture. The increase in reactor diameter results in both increases in buoyancy forces as well as significant increases in reactor cost. To reduce many of the costs associated with large-scale vacuum systems, there is a desire to explore reactor configurations that can be operated at atmospheric pressure where chamber and pump costs can be relatively low.

While there have been a large number of studies of atmospheric pressure CVD (APCVD) of various materials, there have been very few studies that address how the fundamental flow structures that are observed in APCVD change as reactor diameter is increased. This is particularly so for heavier carrier gases for which the buoyancy effects are significantly large. We have recently studied [1,2] the flow patterns and deposition characteristics in a new type of stagnation flow reactor system. In this configuration, shown in Fig. 2, the inlet gases enter the reactor chamber through a narrow inlet with a high momentum. These gases impinge on the heated substrate and flow outwards from the stagnation point to an annular outlet. The distance between the substrate and the upper cover of the reactor is much smaller than in the conventional reactor shown in Fig. 1, thus substantially reducing the buoyancy driven flow. Note the Grashof number (Gr) indicative of the buoyancy force increases as the third power of the characteristic height. Further, the substrate is also rotated, thus accelerating the inlet flow and creating a circumferentially uniform deposition. The buoyancy generated force is counteracted by the momentum of the inlet gases and the forces due to substrate rotation.

In the two previous papers, we have conducted systematic computational studies to understand the effects of the various parameters that influence the rate of deposition as well as its radial uniformity in this new type of CVD reactor. The parameters that were varied included the reactor pressure, substrate rotation rate, inlet flow rate, and reactor thermal boundary conditions in addition to the shape of the reactor itself. A systematic study of the effects of these parameters requires considerable effort experimentally but could be accomplished more easily through computational fluid dynamics [3]. As an initial attempt, we had considered only small wafer sizes (5 cm diameter) to correspond with our experimental facility [4]. These computations demonstrated that highly uniform films (with <1% *rms* variation in film uniformity) are possible with careful selection of the reactor parameters. Our current study assumes fast chemical kinetics. However, if the deposition is limited by the chemical kinetics, the film deposition can be more uniform than the mass transfer limited case. Also, the properties of the film can be influenced by the chemical kinetics and particulate formation above the substrate.

However, scaling up of any CVD reactor from small wafer sizes to larger dimensions provides newer chal-

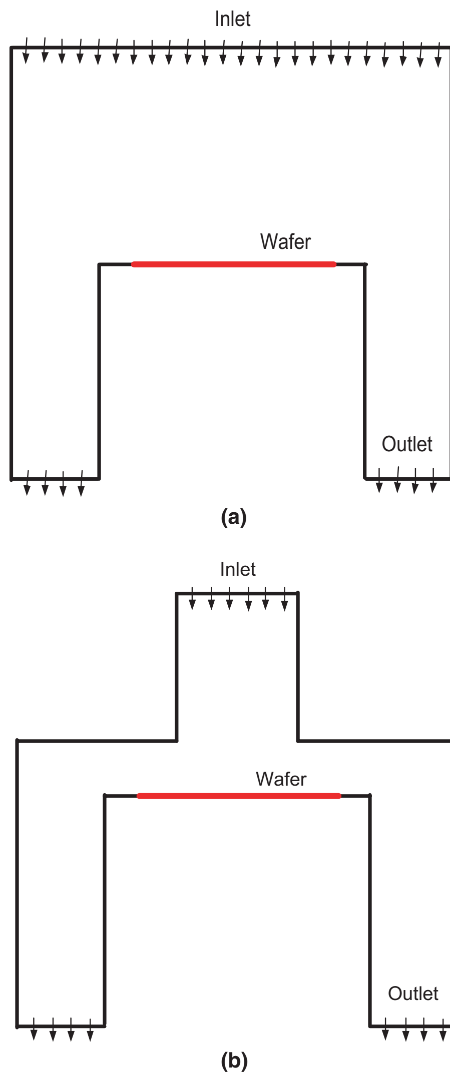

Fig. 1. (a) Schematic of a typical stagnation flow reactor CVD reactor. (b) Schematic of a new impinging jet CVD reactor.

lenges. The buoyancy forces increase considerably as the reactor size or the operating pressure is increased, making the transport of the reactants to the wafer highly complex and non-uniform. A simple linear scaling of all parameters and geometrical dimensions with the wafer size is not expected to produce desired flow patterns and uniformity of the film. The increase in the height of the reactor in proportion with the wafer size increases the Grashof number as the third power of the height, which significantly increases the natural convection velocities, causing complex flow recirculation regions on the top of the substrate. In addition, the flow can become unsteady and even three-dimensional for some parameter combinations. Such situations are detrimental for uniform growth of the film, and must be avoided by appropriately altering the reactor geometry and operating parameters. Hence, further design studies to study the influence of the geometric and flow parameters after scale-up must be carried out.

Since current commercial processes are scaling up to wafer sizes of 30 cm in diameter [5], in the present study we have examined the issue of scaling the reactor design previously observed [1,2] to be optimal for 5 cm wafers, to wafers of 30 cm diameter. A new set of computations has been conducted to understand and modify the behavior of this reactor under scale-up. First, computations were performed in which all reactor dimensions and the flow rate were increased proportionately from the previous optimal design. As these studies did not produce the desired flow patterns and film uniformity, we considered variations to geometry, flow rates and rotational speed of the substrate. We observed that for some combinations of the parameters the flow becomes unsteady. For others, the flow is steady over most of the wafer region. However, in view of the non-uniformity of the deposition pattern, parameters producing unsteady flow were considered not optimal. One source of unsteadiness was the shear layers at the sharp corners of the inlet nozzle and the radial outlet (Fig. 2). These sharp corners make the shear layers unsteady much in the same way as the flow after a sudden expansion. A modification to the geometry in the form of rounded corners was subsequently observed to damp such instabilities.

The present paper discusses the results of these computations aimed towards an acceptable scaled-up version of the impinging jet reactor. We have been successful in determining the geometry and a range of appropriate flow parameters that can provide a deposit of high radial uniformity. We observe that a combination of rotation, lowering of the reactor height and volumetric flow can give films of high quality, opening the doors for large area atmospheric pressure deposition in stagnation flow reactors.

Section 2 first gives a brief overview of the previous studies on transport processes in chemical vapor deposition reactors. This is followed by the governing equations, and a description of the numerical procedure used to solve them. In the present study, the unsteady, axisymmetric Navier–Stokes equations for a variable density flow are numerically solved in conjunction with equations for transport of energy and precursor gas concentration. Section 4 discusses the scale-up of the non-dimensional parameters influencing the flow field. Section 5 first presents results in the scaled-up version of the previously optimized design. Based on the observed flow patterns, the geometry was modified to have rounded corners which stabilized the corner shear layers. Further computations were performed in this geometry to understand the effects of changing the carrier gas

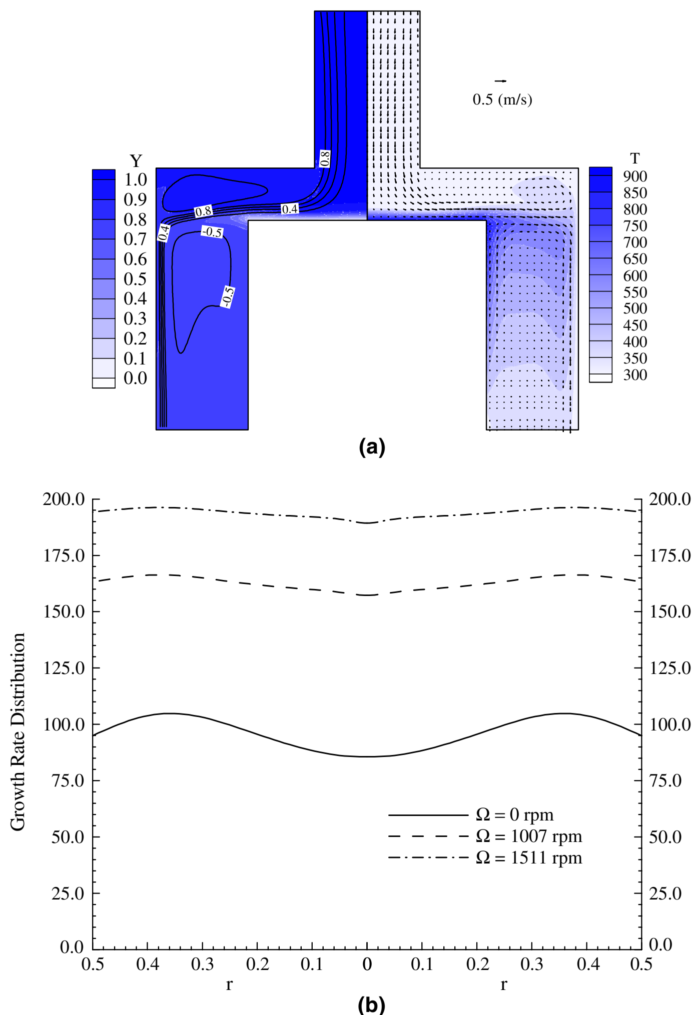

Fig. 2. (a) Streamlines, concentration (left) and temperature (right) contours and vector plot for inlet flow rate = 10 SLM, $\Omega = 0$ rpm, and $d_w = 5$ cm. (b) Growth rate along the wafer at various substrate rotation rates for pressure = 1.0 atm an inlet flow rate = 10 SLM.

flow rate, substrate rotation rate, and the height of the reactor chamber. The last section provides a summary of all these computations.

2. Previous research

A considerable amount of research has been devoted to the understanding of the transport processes in stagnation flow type CVD reactors. These previous works have highlighted the importance of buoyancy-induced flows and reactor shape on film uniformity and growth rate. However because of the reduced buoyancy at low pressures, most of these studies were limited to low pressures. Wang et al. [6] investigated a vertical rotating-disk MOCVD (metal organic CVD) reactor operating at reduced pressure (0.2 atm) using both computations and experiments. They focused on eliminating buoyancy-induced flow and found, in agreement with Evans and Grief [7], that susceptor rotation is a critical parameter. Furthermore, they performed a parametric study of the effects of reactor parameters on thin film uniformity and found that the secondary flows caused by buoyancy effects, reactor shape, forced convection, and substrate rotation can be eliminated by appropriate choice of operating pressure, gas flow and substrate rotation rate, albeit still in a low pressure environment.

Fotiadis et al. [8,9] established through computational studies that the effects of the geometry of the reactor on the deposit uniformity were significant in stagnation flow reactors. They suggest inverting the reactor, shortening distance between inlet and susceptor, introducing baffles, and reshaping reactor wall to mitigate buoyancy effects. Although they looked at several

pressures, they were only able to predict uniform films for pressures much less than atmospheric. The study of Gadgil [10] reached similar conclusions in an experimental study that demonstrated through flow visualization that secondary flows were strongly influenced by the gas inlet configuration though no growth measurements were made. Other experimental work was performed by Kondo and Tanahashi [11] in a study that systematically varied several key reactor parameters to assess their effects on the low pressure CVD environment.

Dilawari and Szekely [12] presented numerical results for a modified stagnation point flow reactor. The major difference between their modified reactor and classical vertical stagnation reactor is that the reactor is inverted and the distance between the inlet showerhead and wafer was reduced to low values. They found that the inverted reactor is helpful in minimizing thermal natural convection and the inlet–wafer distance is critical in obtaining good spatial uniformity of deposition rate in their design. The inlet to wafer distance of 10 mm was seen to provide good spatial uniformity for a diameter of the reactor tube of 200 mm. They argue that the small inlet-to-wafer distance reduces the ability of the carrier gases to entrain fluid from the surroundings thus preventing the formation of the secondary flows.

Cho et al. [13] studied the optimization of inlet concentration profile of the reactant gas on the uniformity of the growth rate. Their results showed that the film uniformity could be significantly improved by enforcing an optimum inlet concentration distribution. However, they noted that controlling the inlet concentration is not easy. To make the optimization procedure more practical, Cho et al. [14] also devised a procedure to find the optimum inlet velocity profile. These calculations showed that a properly arranged inlet velocity profile can suppress buoyancy driven recirculation, thus improving the growth rate uniformity. Several other studies [15,16] also examined the combined effects of forced and free convection on deposit uniformity. The complete reviews are available in Jensen et al. [17], Kleijn et al. [18], and Luo [19].

In contrast with the significant amount of research that is available for low pressure CVD reactors there are fewer studies of fluid flow in CVD reactors at atmospheric pressure. This is primarily because buoyancy driven flows are significantly greater at atmospheric pressure if conventional stagnation flow type reactors are used. Hence much of the interest in CVD reactors has been at low pressures. van Santen et al. [20] proposed that conventional flow reactors can be operated in the turbulent natural convection regime and the deposition rates may be satisfactory in the time-averaged sense. However, controlling film uniformity to the level desired in most microelectronic applications may not be possible in the turbulent regime, especially when the reactants are switched frequently. One industrial atmospheric pressure CVD reactor has been based on the concept of moving the wafer underneath an impinging jet [21]. The rate of deposition underneath the impinging jet is the highest, but decreases significantly with distance away from the point of impingement. As the wafer is moved in the longitudinal direction, the time-averaged deposition rate will be nearly the same, and hence a uniform thin film can be deposited.

Recently [1,2], we had demonstrated that uniform thin films can be grown in small diameter atmospheric pressure stagnation flow type reactors. This reactor, named an impinging jet reactor, carefully balanced the inlet jet momentum with the natural convection flow, to obtain a uniform mass transfer rate. However, these studies were based on a small size reactor (5 cm wafer), and did not explore effects of scaling the reactor size to large wafer dimensions. In view of the current trend to large diameter wafers [5], scale-up of this impinging jet reactor is considered in this paper.

3. Governing equations and numerical procedure

The governing equations and numerical scheme used are essentially the same as those in Refs. [1,2]. Because the velocities encountered in the proposed configuration are small, we consider the flow to be incompressible. However, the density varies with temperature and spatial variations of density are fully accounted for in all the terms without invoking the Boussinesq approximation. The dimensional equations are first non-dimensionalized by using the wafer diameter (d_w) for the length scale, the inlet velocity of the carrier gases (V) for the velocity scale, and the temperature difference $\Delta T_c(T_w - T_{in})$ as the temperature scale. Correspondingly, the pressure is

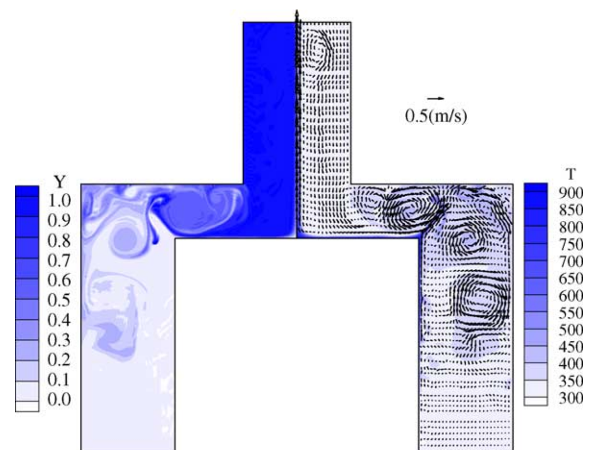

Fig. 3. Concentration (left) and temperature (right) contours and vector plot for inlet flow rate = 360 SLM, $\Omega = 0$ rpm, and $d_w = 30$ cm.

non-dimensionalized by $\rho_{ref}V^2$ and time by d_w/V. The non-dimensional governing equations can then be written as [22]:

$$\frac{\partial \rho}{\partial t} + \nabla \cdot (\rho \mathbf{u}) = 0 \tag{1}$$

$$\frac{\partial \rho \mathbf{u}}{\partial t} + \nabla \cdot (\rho \mathbf{u}\mathbf{u}) = -\nabla p + \frac{1}{Re_w} \nabla \left\{ \mu \left[\nabla \mathbf{u} + (\nabla \mathbf{u})^{Tr} - \frac{2}{3}(\nabla \mathbf{u}) \cdot I \right] \right\} + \frac{Gr_w}{Re_w^2} \left[\frac{\Theta - 1/2}{(\Theta - 1/2)Ga + 1} \right] \mathbf{e}_x \tag{2}$$

$$C_p \frac{\partial \rho \Theta}{\partial t} + C_p \nabla \cdot (\rho \mathbf{u} \Theta) = \frac{1}{Re_w \cdot Pr} \nabla \cdot (k \nabla \Theta) \tag{3}$$

$$\frac{\partial \rho Y}{\partial t} + \nabla \cdot (\rho \mathbf{u} Y) = \frac{1}{Re_w \cdot Sc} \nabla \cdot (\rho D \nabla Y) \tag{4}$$

Here $\mathbf{u}$ is the velocity vector, $\mathbf{I}$ is the unit tensor, $\mathbf{e}_x$ is the unit vector with component only in the x direction (positive x direction points upwards), and p is pressure. The superscript Tr indicates transpose of the tensor. Θ and Y are the non-dimensional temperature and the mass fraction of precursor gas respectively, and t is the time. All variables are non-dimensional. The material properties, density ρ, dynamic viscosity μ, thermal conductivity k, heat capacity C_p, and the mass diffusivity D are made dimensionless with their value at the reference temperature $T_{ref} = (T_w + T_{in})/2$. The Reynolds ($Re_w$), Prandtl ($Pr$), Schmidt ($Sc$), Grashof ($Gr_w$), and Gay-Lusac ($Ga$) numbers appearing in the above equations are defined as

$$\begin{aligned} Re_w &= \rho_{ref} V d_w / \mu_{ref}, \quad Pr = \mu_{ref} C_{p_{ref}} / k_{ref} \\ Sc &= \mu_{ref} / (\rho_{ref} D_{ref}) \\ Gr_w &= g \rho_{ref}^2 d_w^3 (T_w - T_{in}) / (\mu_{ref}^2 T_{ref}) \\ Ga &= (T_w - T_{in}) / T_{ref} \end{aligned} \tag{5}$$

where g is the acceleration due to gravity, T_w and T_{in} represent dimensional temperatures at the wafer and at the inlet. Reference values denoted by the subscript ref are taken at reference temperature. Expansion effects caused by density changes with heating of the gas phase are modeled by the ideal gas law. This gives the following dimensionless relation.

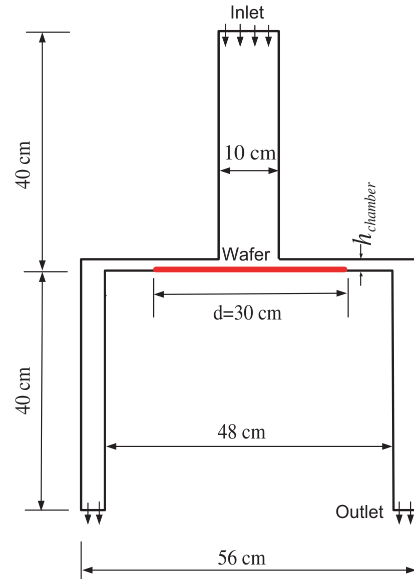

Fig. 4. Schematic of the modified CVD reactor with sharp corners.

$$\rho = [(\Theta - 1/2)Ga + 1]^{-1} \tag{6}$$

For the present computations, we have used argon and acetone as the carrier and precursor gases respectively. The relevant properties of these two gases were obtained from database of National Institute of Standards and Technology (NIST) [23]. The wafer temperature was taken to be 900 K and the inlet gases were at 300 K. The binary diffusion coefficients were calculated from the Chapman–Enskog theory. The Dufour and Soret diffusion are assumed to be small for the particular gases considered here, and hence they have been neglected in the equations. In the above equations, we have made the explicit assumption that the flow is axisymmetric. This assumption reduces the computational burden significantly. However, for certain parametric combinations the flow may become three-dimensional. van Santen et al. [24,25] recently studied mixed convection between two circular plates with a central jet. Their experimental and numerical studies showed that the flow can become three-dimensional and unsteady when the Rayleigh number exceeds a critical value for a given inlet

Table 1
Details of calculation parameters

h (cm)	Grashof number based on h	Volumetric flow rate (SLM)	Inlet Reynolds number based on 10 cm	V_{in} (cm/s)	Gr/Re_{in}^2
2.0	33,935.51	360	1589.4	0.764	0.013
2.0	33,935.51	180	794.7	0.382	0.053
4.0	27,1484.1	360	1589.4	0.764	0.107
4.0	27,1484.1	180	794.7	0.382	0.430

Reynolds number and the fluid Prandtl number. These were in the case of no substrate rotation and no radial confinement of the flow. The flow characteristics can be significantly different with substrate rotation, variable properties and outer wall confinement.

It is also logical to assume that three-dimensionalities in the flow will only worsen the radial uniformity and not improve it. Hence, the present calculations can be first used as a means to select the best combinations of parameters for which full three-dimensional calculations should be eventually performed to confirm the axisymmetric solutions. This may especially be the case when the axisymmetric flow computation predicts an unsteady solution. Nevertheless, because of rotation of the wafer, the growth pattern averaged in azimuthal direction will still be axisymmetric.

The boundary conditions for the solution of the above equation were as follows. At the top surface the velocities and concentration values corresponding to the inflow gases are prescribed as Dirichlet conditions. At the wafer, the non-dimensional temperature is fixed at unity, and the non-dimensional concentration is prescribed to be zero. The normal and radial velocities are also prescribed to be zero at the wafer surface with the tangential velocity prescribed by the rotation rate. At the outlet of the reactor, zero-derivative conditions are prescribed on all variables. The temperature at the outer wall is an important aspect for the operation of the reactor. It is necessary to select this in such a way that there is no deposit on the outer wall, but at the same time the buoyancy forces due to the cold outer walls are mitigated. As in our previous studies [1,2], we considered the outer wall to be an isothermal wall at 300 K, implying some form of external cooling to maintain the walls at the temperature of the inlet gases. The pedestal side wall is stationary and a linear temperature difference

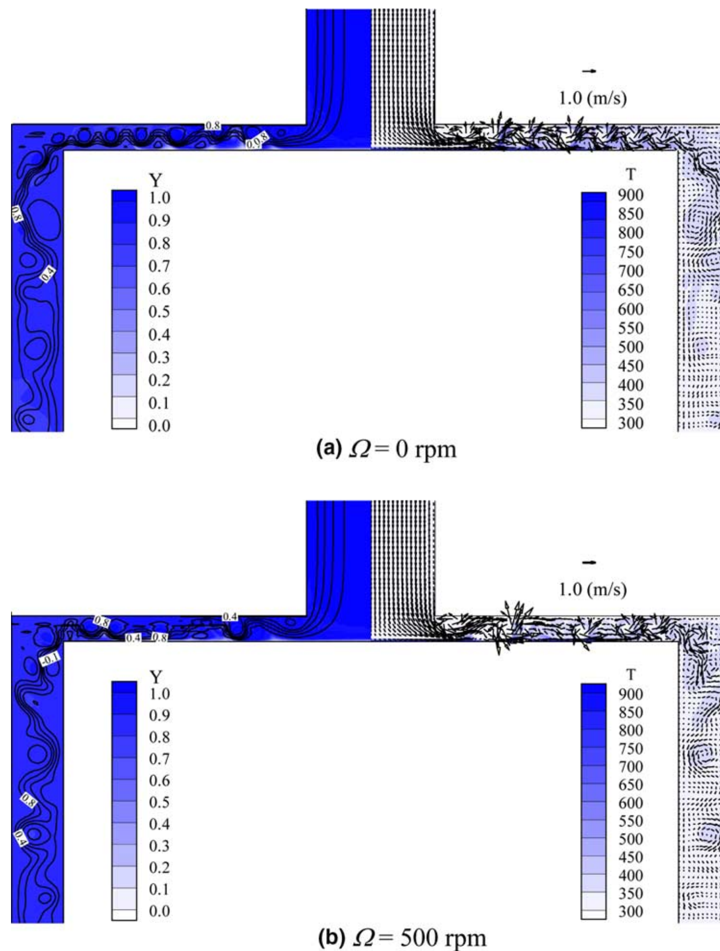

Fig. 5. (a) Streamlines, concentration (left) and temperature (right) contours and velocity vectors for inlet flow rate = 360 SLM at a time instant. (b) Growth rates along the wafer at different substrate rotation rates for inlet flow rate = 360 SLM, $h = 2$ cm, and sharp corners.

from the wafer surface temperature (900 K) to the ambient of 300 K was prescribed. We believe this condition will not affect the deposition patterns on the wafer. Other conditions appropriate to an industrial setting may be considered in future studies.

The rate of deposition is assumed to be limited by the rate of mass transfer, implying fast chemical kinetics. Thus the growth rate is taken to be proportional to the gradient of the concentration normal to the wafer surface (Growth rate $\propto Sh = -\partial Y/\partial x|_{\mathrm{w}}$). The growth rate is

Table 2
Growth rates and non-uniformities for the impinging jet CVD reactor

	Inlet flow rate (SLM)	Rotation speed (rpm)	Average growth rate	rms non-uniformity (%)	Usage(%)
Sharp corners	360	0	143.98*	11.64*	13.09*
		200	150.12*	10.37*	13.65*
		500	153.08*	9.01*	13.92*
		800	–	–	–
Rounded corners	360	0	73.89	27.38	6.71
		200	90.62	14.14	8.23
		500	122.09	5.21	11.09
		800	150.04	2.64	13.64
Rounded corners double height	360	0	–	–	–
		200	92.51*	12.31*	8.40*
		500	121.73*	4.77*	11.06*
		800	149.70*	2.30*	13.61*
Rounded corners	180	0	–	–	–
		200	78.60	7.83	14.29
		500	115.57	2.14	21.01
		800	145.57	1.01	26.46
Rounded corners double height	180	0	–	–	–
		200	79.66*	7.93*	14.47*
		500	115.47*	1.89*	21.00*
		800	145.49*	0.95*	26.45*

Note: (1) *Means time-averaged value. (2) – means that there is no 2D solution.

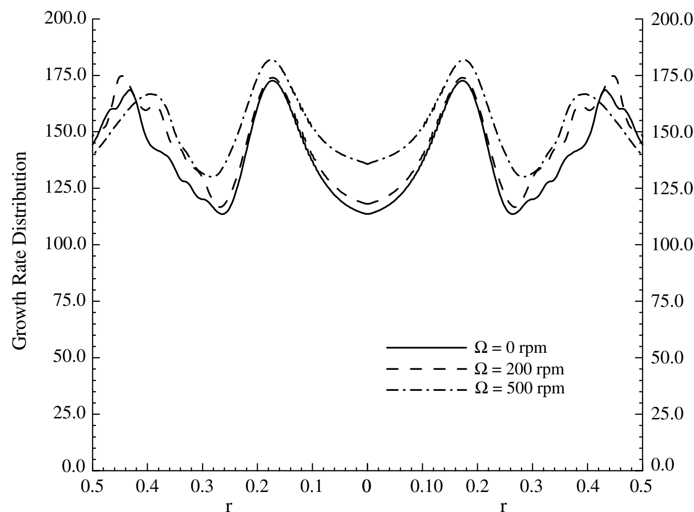

Fig. 6. Growth rates along the wafer at different substrate rotation rates for inlet flow rate = 360 SLM and h = 2 cm and sharp corners.

given by the product of the local density, diffusion coefficient and the concentration gradient. In our study, the radial variations of density and diffusion coefficients near the wafer are small because of the dilute concentrations of the precursor and uniform wafer temperature. When the deposition rate is limited by the kinetics of the reaction, it is necessary to include the specific kinetic mechanisms before actual film deposition rates are estimated. By appropriately specifying a value to the inlet concentration, a dimensional value can be then obtained. Hence the units for current growth rates are arbitrary. We also calculate the fraction of precursor that reacts at the surface, and we call this fraction the usage. The non-uniformity and usage are defined as the following:

$$\text{Non-unifomity} = \left\{ \int_{A_w} (Sh - \overline{Sh})^2 \mathrm{d}A / \overline{Sh}^2 A_w \right\}^{1/2} \tag{7}$$

where $\overline{Sh} = \int_{A_w} Sh\, \mathrm{d}A/A_w$ is the average growth rate and A_w is the area of the wafer.

$$\text{Usage} = \frac{\int_{A_w} \rho D (\partial Y/\partial x)_w \mathrm{d}A}{\int_{A_{in}} \rho V Y_{in} \mathrm{d}A} \tag{8}$$

4. Scale-up issues

Scale-up of any reactor to larger wafer sizes brings new complexities to the flow. A non-dimensional analysis of the scale-up shows the following trends. If the mixed convection parameter is based on the inflow jet momentum and the Grashof number based on chamber height (not the wafer diameter as in Eq. (2)), then

$$Re_{in} = \rho_{in} V_{in} d_{in} / \mu_{in} \propto \dot{m}_{in} / d_{in} \tag{9}$$

If the carrier gas volume flow per unit area of the wafer (m_{sp}) is kept the same,

$$Re_{in} \propto m_{sp} d_w^2 / d_{in} \propto d_w^2 / d_{in} \tag{10}$$

The Grashof number is given by

$$Gr_h = g \rho_{ref}^2 h^3 (T_w - T_{in}) / (\mu_{ref}^2 T_{ref}) \propto h^3 \tag{11}$$

This mixed convection parameter (Gr_h/Re_{in}^2) scales as:

$$Gr_h/Re_{in}^2 \propto h^3 d_{in}^2 / d_w^4 \tag{12}$$

For the optimal design of the 5 cm wafer reactor [1,2], the mixed convection parameter (Gr_h/Re_{in}^2) was 1.191, a value around unity. Hence, forced convection in this reactor was significant. If we scale all the dimensions of this reactor proportionately from the 5 cm size to 30 cm, the mixed convection parameter will increase sixfold to 7.418. As this is large, it is likely that the natural convection effects will become significant at this reactor size if all dimensions and flow rate are linearly scaled.

In addition to the above defined mixed convection parameter, another mixed convection parameter appropriate to the boundary layer flow region has also been previously suggested [25]. This is based on the ratio of the momentum of the wall jet boundary layer and the natural convection force above the wafer. In a horizontal CVD reactor [24] a scale-up criterion which varies as the inverse of the first power of the Reynolds number was proposed to be more appropriate. The Reynolds number in this case is defined as:

$$Re_h = \rho V_h h / \mu \propto \dot{m}_{in} h / 2\pi R h \propto \dot{m}_{in} / R \propto d_w^2 / R \tag{13}$$

with the mixed convection parameter calculated at wafer edge given by

$$Gr_h / Re_h = h^3 / d_w \tag{14}$$

If we scale all dimensions (including chamber height) proportionately from the 5 cm design to the 30 cm design, this second mixed convection parameter Gr_h/Re_h increases 36-fold. Thus both the criteria (Gr_h/Re_{in}^2 and Gr_h/Re_h) imply that straightforward scaling of the reactor based on wafer diameter may result in unfavorable flow fields for uniform deposition. This has been confirmed by our current study, which led us to modify the geometry and flow parameters.

5. Results

5.1. Initial scale-up

We first present a few results of the previously optimized 5 cm wafer reactor. Fig. 2(a) shows the velocity field

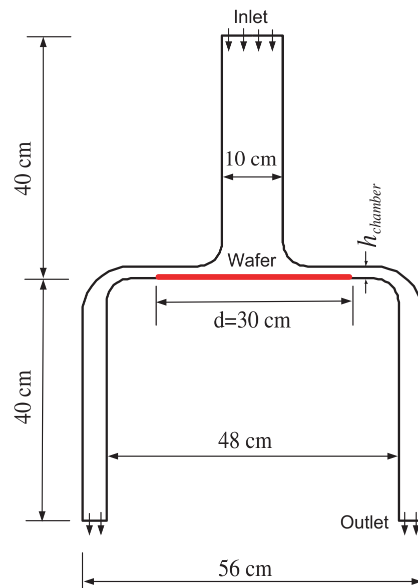

Fig. 7. Schematic of the modified CVD reactor with round corners.

and concentration contours for a flow rate of 10 SLM and with no rotation of the substrate. The height of the reactor and the inlet diameter of the gases were 1.69 and 3.38 cm. Fig. 2(b) shows the mass transfer limited growth rate computed as a function of the radial distance. It is seen that with increasing rotation, not only does the growth rate increase, but the profile becomes very uniform. It is this advantageous feature that led us to consider further scale-up of this configuration.

As an initial scale-up we first considered increasing all dimensions of the reactor in proportion to the wafer size, and the flow rate in proportion with the wafer surface area. This configuration is shown in Fig. 3, along with an instantaneous snapshot of flow, temperature and scalar fields. It is first observed that there is no steady solution to the governing equations. Several unsteady vortices are observed above the wafer and in the annular passage at the exit. These unsteady vortices can be a result of either the instability of the shear layer or of the buoyant vortices. In addition, instabilities may also result from the rotation of the substrate. The impact of this unsteadiness on the deposition is unfavorable, as it results in large radial non-uniformities.

Subsequent computations were aimed at first reducing the buoyancy force, by decreasing the height of the reactor. Since the Grashof number varies as the third power of the height, computations were performed with a reduced height. In the linear scaling, this height was also scaled in proportion with the wafer size. However, such an increase is not necessary from any transport view point. Hence the first set of new computations was performed with a height of 2 cm which is close to the previous value in the 5 cm wafer reactor. The reactor configuration with this change is shown in Fig. 4. All relevant lengths are non-dimensionalized by the wafer diameter d_w (30 cm). The susceptor diameter is 36 cm. The inlet gases enter through the nozzle and turn sharply at the corners to form a radial wall jet. The radial jet

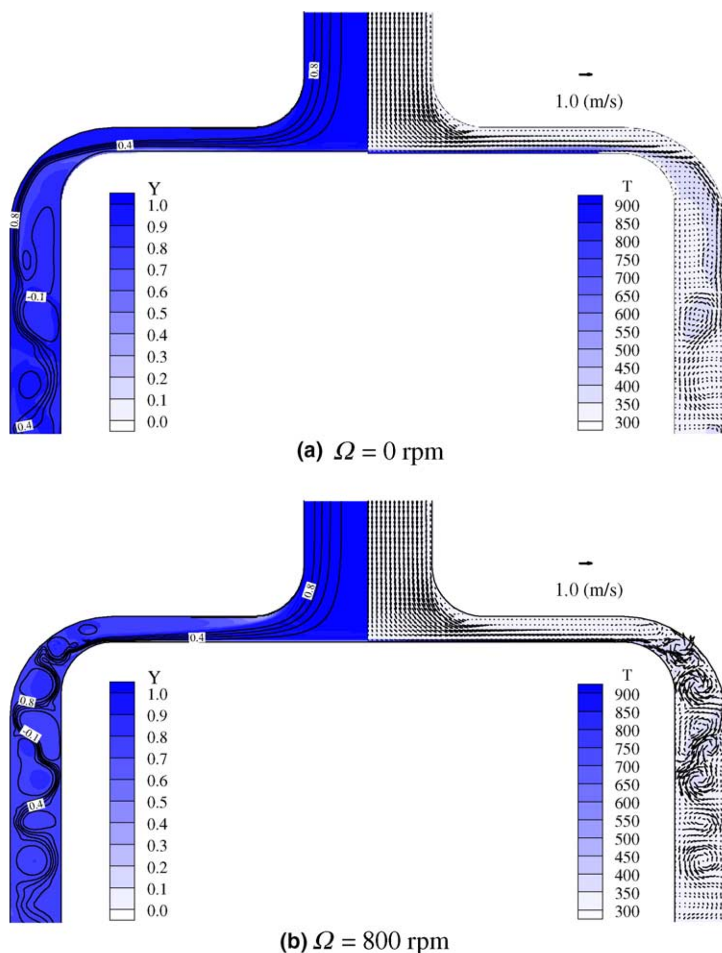

Fig. 8. Streamlines, concentration (left) and temperature (right) contours and velocity vectors for inlet flow rate = 360 SLM at a time instant.

convects away the natural convection cells, avoiding recirculation above the wafer. As the flow moves along the radial coordinate, the momentum of the jet decreases due to area expansion.

A finite volume grid containing 33,462 cells was used to discretize the governing equations. The grid spacing was uniform in the radial direction, but a non-uniform spacing, symmetrically expanding from the substrate towards the inlet and outlet boundary, was employed in the axial direction. The time step was chosen as a value which guaranteed the maximum Courant number at all control volumes to be less then 0.8. The steady state solution was considered to be reached when the sum of the temporal derivatives of density of all control volumes over the entire domain became less then 10^{-7}.

Computations in this geometry were done for a flow rate of 360 SLM, which is a direct scaling of the 10 SLM flow at 5 cm wafer size. Four computations with zero, 200, 500 and 800 rpm were performed. However, it was observed that the calculations did not attain a time asymptotic state. Instead, the flow was observed to be periodic, and the deposition rates fluctuated in time. However, these deposition rates can be averaged in time to get a time-mean deposition pattern. These growth rates and the rms non-uniformities of the deposition profiles are given in Table 2.

The above non-uniformities are unacceptable for high-end applications. In Table 1, we have given the corresponding non-dimensional parameters, the Grashof number, the Reynolds number, and the mixed convection parameter (Gr_h/Re_{in}^2). The mixed convection parameter for these computations was quite small around 0.013. This is because the Grashof number now is nearly the same as in the small reactor, while the Reynolds number increased significantly. Thus the source of the observed instability cannot be the natural convection. A closer look at the instantaneous flow field and its animation revealed that vortices are continuously shed from the shear layer at the corner of the inlet and the radial gap (Fig. 5(a)). The flow over the wafer is seen to consist of multiple traveling vortices that have nearly the same size. Thus the source of the instability was concluded to be the shear layer and not the natural convection. Because of the significant increase in the Reynolds number of the inlet jet, we believe that we have exceeded the critical Reynolds number for a stable shear layer in this configuration. However, only a rigorous stability analysis can determine the precise critical Reynolds number. Fig. 5(b) shows the results for a case with 500 rpm rotation. The time-averaged RMS film non-uniformity is around 11%. The rotation induced pump action has little effect on the film uniformity and deposition rate. The average growth rate increases only 6.32% as the rotation rate increases from 0 to 500 rpm. The time-averaged RMS non-uniformity decreases from 11.64% to 9.01% as the rotation rate increases from 0 to 500 rpm (Table 2). Fig. 6 shows the time-averaged deposition rate profiles for different rotation rates. As the rotation rate is increased to 800 rpm, no solution was possible to the axi-symmetric flow equations. It is suspected that the flow may be three-dimensional, which may have caused the numerical solution to diverge. Since our analysis shows that in this design the mixed convection parameter is much less that of the 5 cm design, the unsteadiness is not caused by the buoyancy force. Also, a cold gas simulation, in which a uniform temperature of 300 K is prescribed everywhere, still shows a similar unsteady flow pattern. Thus, we

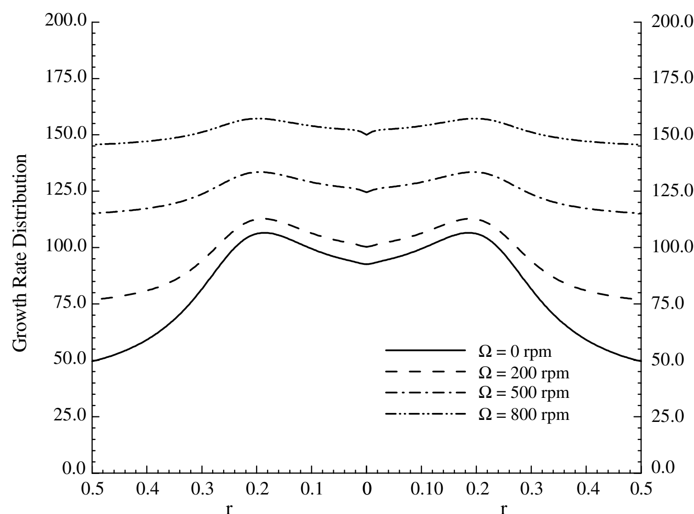

Fig. 9. Growth rates along the wafer at different substrate rotation rates for inlet flow rate = 360 SLM and $h = 2$ cm.

concluded that the unsteady flow field is caused by the sharp 90° corner. The sudden turning of the flow makes the shear layer unsteady.

It is also seen that the instability does not diminish with rotation. This is expected because rotation accelerates the inflow to the wafer, making the corner vorticity larger. Since the unsteady behavior of the flow is detrimental to the deposition uniformity it is necessary to consider variants to this geometry.

5.2. Rounded corners

A cure for the shear layer instability may be to modify the sharp corners to be less abrupt. Rounding the corners can streamline the corner flow. One such modified geometry is shown in Fig. 7. The radii of the small and large round corners are 4 and 8 cm respectively. The radius of these turns is somewhat arbitrary, but has been selected proportional to the height of the chamber. Too small a value may not remove the instability, while a large value may diffuse the flow too much, in an adverse way.

Computations for this configuration were performed for four rotation rates. The observed flow fields for zero and 800 rpm are shown in Fig. 8. Interestingly, it is observed that the rounded corners have a large impact on the flow field and film uniformity. The rounded corners have suppressed the unsteadiness and the flow over the wafer has now become steady, although the flow in the exit annular passage still contains unsteady vortices. These vortices become stronger with rotation, but do not appear over the wafer even with rotation. Their

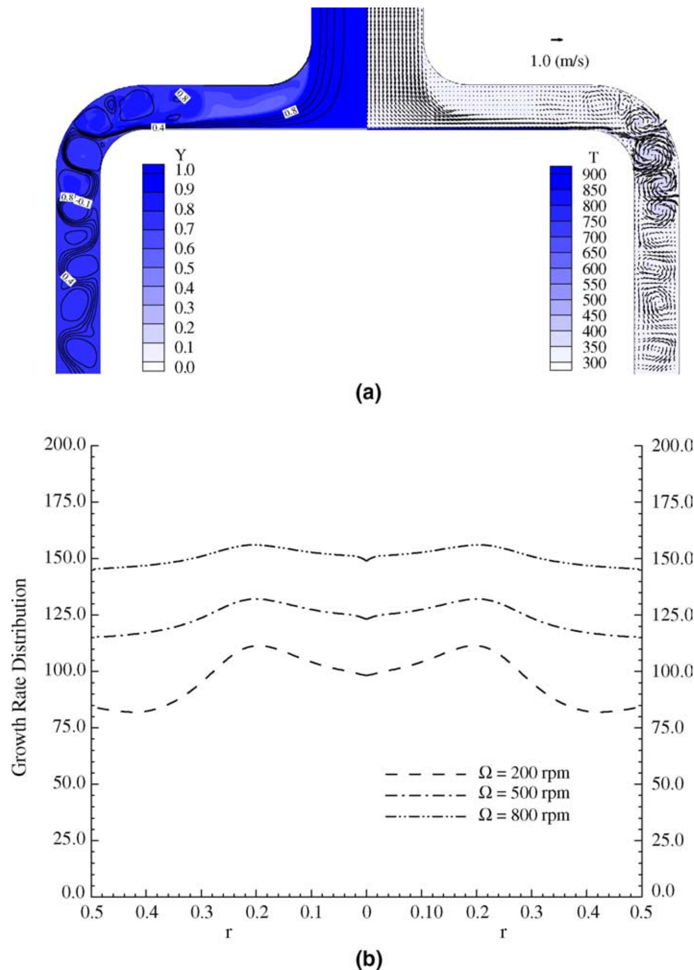

Fig. 10. (a) Streamlines, concentration (left) and temperature (right) contours and velocity vectors for inlet flow rate = 360 SLM, $h = 4$ cm, and $\Omega = 800$ rpm at a time instant. (b) Growth rates along the wafer at different substrate rotation rates for inlet flow rate = 360 SLM and $h = 4$ cm.

effects are confined to the downstream. Thus it is apparent that the previously observed instabilities arose due to the corner shear layer.

The growth rate and pattern for the four computations are shown in Fig. 9. For zero rotation, the deposition is non-uniform with two humps and a dip in the center. As the substrate is rotated, the profile becomes more uniform, and the concentration gradients become steeper. At the highest rotation rate of 800 rpm, the profile is quite uniform, but some further optimization is still possible. As expected, the increased rotation rates increase the concentration gradients. The growth rate is doubled by rotating the substrate at 800 rpm. As shown in Table 2, the RMS non-uniformity decreases monotonically with the rotation rate of the substrate. It is seen that at 800 rpm, the deviation from uniformity is only about 2.64%, which is quite good for high-end applications. The usage is seen to increase with rotation, up to 14% from 6.7% at zero rotation.

It is therefore clear that modifying the shape of the reactor can make the flow stable and uniform. Further improvements in growth rates may be possible by changing the height of the reactor and the flow rate of the carrier gases. Since a complete optimization requires considerable computational effort, we show below only two sets of additional calculations in which the height and the inflow have been varied. For these calculations we have used the rounded corner design.

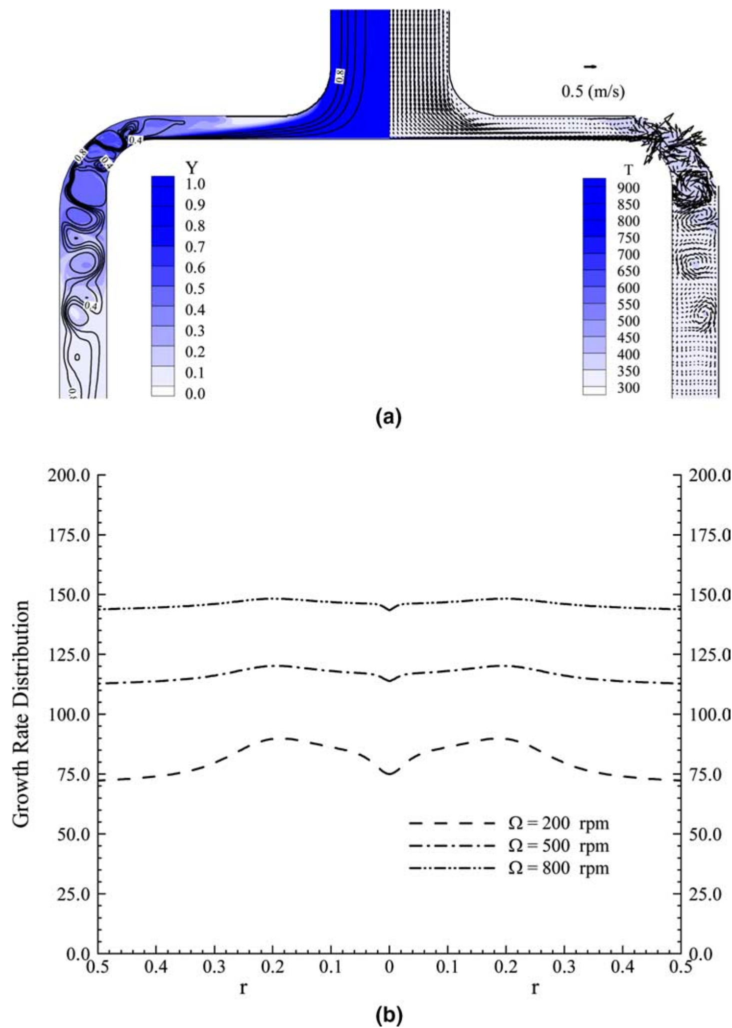

Fig. 11. (a) Streamlines, concentration (left) and temperature (right) contours and velocity vectors for inlet flow rate = 180 SLM and $\Omega = 800$ rpm at a time instant. (b) Growth rates along the wafer at different substrate rotation rates for inlet flow rate = 180 SLM and $h = 2$ cm.

5.3. Effect of chamber height

The chamber height is one of the key geometric parameters that influence the flow field and the deposit uniformity. A systematic optimization is in principle possible but computationally quite expensive. In order to study the sensitivity of the deposition pattern to the reactor height, we considered four new computations with a height of the chamber of 4 cm (double the previous height). However, the choice of this value was arbitrary and other values could have also been chosen.

Computations were performed with a grid consisting of 40,096 cells for four rotation rates (0, 200, 500 and 800 rpm). For the case of zero rotation, we observed that the flow was unsteady, and eventually the calculation diverged. Despite reducing the time step size, no stable solution was found. For the other three rotation rates, unsteady, periodic solutions were obtained but the unsteadiness was primarily in the annular exit region. Fig. 10(a) shows the instantaneous flow field for a rotation rate of 800 rpm. The region above the wafer was steady, resulting in a steady concentration field and a deposition rate. As the flow moves outward, the velocity decreases to conserve mass. The unsteadiness observed towards the edge of the wafer may be a result of the natural convection that becomes stronger with doubling of the height (the Grashof number increased eightfold).

Although the flow above the wafer is partially unsteady, the growth rates can be averaged in time to get a mean deposition pattern. For a rotation rate of 800 rpm, the non-uniformity is only 2.3%, which is even lower than the corresponding baseline case with the height of 2 cm (Fig. 10(b)). The growth rates and pattern are however only marginally influenced by doubling the height (Table 2). However, further increases in height may not produce the same conclusion.

5.4. Effect of carrier gas flow rate

The previous sets of calculations were performed for a flow rate of 360 SLM, which was determined by a linear scaling of the mass flow rate with wafer surface area. However, the 10 SLM flow rate of the small wafer size was itself arbitrarily obtained. In the previous studies, it was found to give good uniformity over the other value tested, namely 1 SLM. However, it is quite likely that in-between flow rates may also give good uniformity while reducing the consumption of carrier gases and increasing precursor usage. With this in mind, another two sets of calculations were conducted with half the volumetric flow rate (180 SLM) for the two heights considered. Again, four rotation rates (0, 200, 500 and 800 rpm) were considered. Of these calculations, the zero rotation case was not stable. The flow field for 800 rpm is shown in Fig. 11(a). This flow was steady on most of the wafer, but was unsteady near the exit. The time-averaged growth rates are shown in Figs. 11(b) and 12. We see that with the 180 SLM flow rate, the non-uniformity decreases from that of the 360 SLM case while the usage almost doubles. The same is observed for the 4 cm height reactor, although the flow was observed to be unsteady over part of the wafer. Thus, lowering the flow rate appears to be quite advantageous. In view of the required computational effort, further test cases were not considered. However, a systematic study to determine the optimum parameters and reactor dimensions

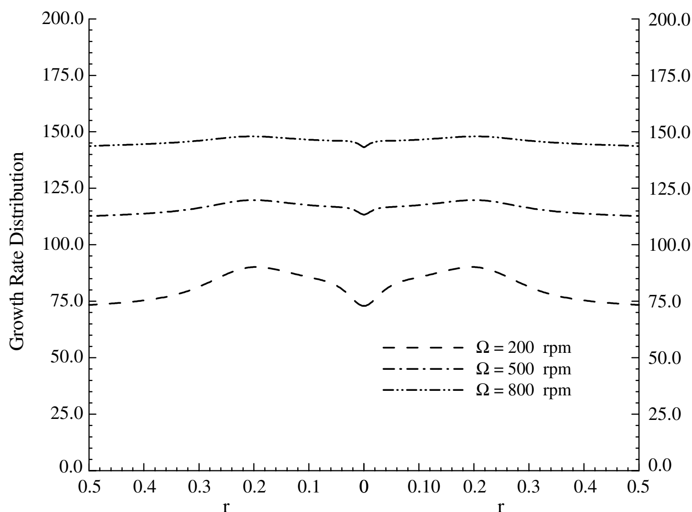

Fig. 12. Growth rates along the wafer at different substrate rotation rates for inlet flow rate = 180 SLM and $h = 4$ cm.

is necessary and should be conducted in future with faster converging algorithms [26].

6. Summary

The objective of our current study was to investigate the scale-up issues of a previously developed design of an atmospheric pressure CVD reactor, which showed promise of depositing highly uniform thin films. The principal feature of the reactor was a high momentum impinging jet that counteracted the buoyancy-induced flows over the wafer. However, scale-up of this design to wafer sizes up to 30 cm in diameter that are of interest to industry is not straightforward. The flow field can become very complex because of the appearance of new instabilities not present at small sizes.

A number of computations have been performed beginning with a simple linear scale-up of the flow rate and the dimensions. However, such a scale-up was not satisfactory. Subsequent modifications to the reactor dimensions and shape were made to arrive at a satisfactory growth pattern. Based on this design, further sensitivity tests were performed by increasing the chamber height and reducing the inlet flow rate. The effect of wafer rotation was studied in all cases.

From the present study, it is clear that an atmospheric pressure stagnation flow reactor with large wafer size can be developed for depositing highly uniform thin films. This is very encouraging since such a reactor system will be much cheaper than those requiring a vacuum system.

The present reactor can be further optimized by exploring smaller flow rates and tailored inflow profiles such that the precursor usage will be high and the non-uniformity will be even smaller than the values currently computed. Such studies should be conducted in future after developing faster converging numerical schemes for steady flows. In addition, it will be necessary to couple finite rate reaction schemes for the concerned species to include their effect in cases when the deposition is rate limited.

Acknowledgment

This work was partly supported by the National Science Foundation grants DMI-0099748 and CTS-03-04132 NER.

References

[1] S.P. Vanka, G. Luo, N.G. Glumac, Parametric effects on thin film growth and uniformity in an atmospheric pressure impinging jet CVD reactor, J. Cryst. Growth 267 (1–2) (2004) 22–34.
[2] S.P. Vanka, G. Luo, N.G. Glumac, Numerical study of mixed convection flow in an impinging jet CVD reactor for atmospheric pressure deposition of thin films, ASME J. Heat Transfer (2004), in press.
[3] Y.K. Chae, Y. Egahira, Y. Shimogaki, K. Sugawara, H. Komiyama, Chemical vapor deposition reactor design using small-scale diagnostic experiments combined with computational fluid dynamics simulations, J. Electrochem. Soc. 146 (1999) 1780–1788.
[4] J. Abon, Chemical Vapor Deposition and Characterization of Titania Photocatalytic Films, Master's thesis, University of Illinois, Urbana-Champaign, IL, 2003.
[5] E.J. McInerney, T.M. Pratt, A. Taheri, Design of a 300 mm chemical vapor deposition tungsten reactor using computational fluid dynamics, J. Vac. Sci. Technol. 17 (1999) 1352–1355.
[6] C.A. Wang, S. Patnaik, J.W. Caunt, R.A. Brown, Growth characteristics of a vertical rotating-disk OMVPE reactor, J. Cryst. Growth 93 (1988) 228–234.
[7] G.H. Evans, R. Greif, A numerical model of the flow and heat transfer in a rotating disk chemical vapor deposition reactor, Trans. ASME 109 (1987) 928–935.
[8] D.I. Fotiadis, A.M. Kremer, D.R. McKenna, K.F. Jensen, Complex flow phenomena in vertical MOVCD reactors: effects on deposition uniformity and interface abruptness, J. Cryst. Growth 85 (1987) 154–164.
[9] D.I. Fotiadis, S. Kieda, K.F. Jensen, Transport phenomena in vertical reactors for metalorganic vapor phase epitaxy, J. Cryst. Growth 102 (1990) 441–470.
[10] P.N. Gadgil, Optimization of a stagnation point flow reactor design for metalorganic chemical vapor deposition by flow visualization, J. Cryst. Growth 134 (1993) 302–312.
[11] Makoto Kondo, Toshiyuki Tanahashi, Dependence of carbon incorporation on crystallographic orientation during metalorganic vapor phase, epitaxy of GaAs and AlGaAs, J. Cryst. Growth 145 (1–4) (1994) 390–396.
[12] A.H. Dilawari, J. Szekely, A mathematical representation of a modified stagnation flow reactor for MOCVD applications, J. Cryst. Growth 108 (1991) 491–498.
[13] W.K. Cho, D.H. Choi, M.-U. Kim, Optimization of the inlet concentration profile for uniform deposition in a cylindrical chemical vapor deposition chamber, Int. J. Heat Mass Transfer 42 (1999) 1141–1146.
[14] W.K. Cho, D.H. Choi, M.-U. Kim, Optimization of the inlet velocity profile for uniform epitaxial growth in a vertical metalorganic chemical vapor deposition reactor, Int. J. Heat Mass Transfer 42 (1999) 4143–4152.
[15] G.H. Evans, R. Greif, Forced flow near a heated rotating disk: a similarity solution, Numer. Heat Transfer 14 (1988) 373–387.
[16] S. Patnaik, R.A. Brown, C.A. Wang, Hydrodynamic dispersion in rotating-disk OMVPE reactors: numerical simulation and experimental measurements, J. Cryst. Growth 96 (1989) 153–174.
[17] K.F. Jensen, E.O. Einset, D.I. Fotiadis, Flow phenomena in chemical vapor deposition of thin films, Annu. Rev. Fluid Mech. 23 (1991) 197–232.
[18] C.R. Kleijn, K.J. Kuijilaars, M. Okkerse, H. van Santen, H.E.A. van den Akker, Some recent developments in

chemical vapor deposition process and equipment modeling, J. Phys. IV 9 (Pr8) (1999) 117.

[19] G. Luo, Study of Buoyancy-induced Flows in a Prototypical CVD Reactor, PhD thesis, University of Illinois, Urbana-Champaign, IL, 2003.

[20] H. van Santen, C.R. Kleijn, H.E.A. van den Akker, On turbulent flows in cold-wall CVD reactors, J. Cryst. Growth 212 (2000) 299–310.

[21] 5500 Series Atmospheric Pressure CVD Systems, retrieved 30 December 2003 from http://www.sierratherm.com/prod5500.htm.

[22] H. van Santen, C.R. Kleijn, H.E.A. van den Akker, Symmetry breaking in a stagnation-flow CVD reactor, J. Cryst. Growth 212 (2000) 311–323.

[23] Database of the Thermophysical Properties of Gases Used in the Semiconductor Industry, retrieved 7 June 2002 from http://properties.nist.gov/SemiProp/Gases/Index.html.

[24] H. van Santen, C.R. Kleijn, H.E.A. van den Akker, Mixed convection in radial flow between horizontal plates. I. Numerical simulations, Int. J. Heat Mass Transfer 43 (2000) 1523–1535.

[25] H. van Santen, C.R. Kleijn, H.E.A. van den Akker, Mixed convection in radial flow between horizontal plates. II. Experiments, Int. J. Heat Mass Transfer 43 (2000) 1537–1546;
E.P. Visser, C.R. Kleijn, C.A.M. Govers, C.J. Hoogendoorn, L.J. Giling, Return flows in horizontal MOVCD reactors studied with the use of TiO_2 particle injection and numerical calculations, J. Cryst. Growth 94 (1989) 929–946.

[26] R. Jyotsna, S.P. Vanka, Multigrid calculation of steady, viscous flow in a triangular cavity, J. Comput. Phys. 122 (1995) 107–117.